Computational Analysis of Mixing and Scale-Up in Emulsion Polymerization Reactors

Jordan Pohn,[1] *Mourad Heniche,*[2] *Louis Fradette,*[2] *Michael Cunningham,*[1] *Timothy McKenna**[1]

Summary: A hybrid multi-zonal/computational fluid dynamics (CFD) framework is currently being developed to aid in the scale-up of high solid content latex production and processing. Poly3D, a commercial laminar CFD code tailored to modelling the mixing of non-Newtonian fluids, has been coupled to a population balance model via a customized interface. CFD is used to generate flow fields inside a series of reactors; this information is then transferred to a multi-zone population balance model to assess the impact of non-homogenous mixing on the evolution of the latex particle size distribution (PSD) when concentrated latex suspension is altered via the addition of a coagulant. The rheological properties of high solid content latexes are sensitive to changes in the PSD, so the flow field is periodically updated if significant changes in the rheological properties of the latex are detected in any of the zones. The details of the models comprising the framework are presented and the utility of the framework is demonstrated.

Keywords: computational fluid dynamics; high solid content latexes; kinetics (polym.); particle size distribution; polymer latexes

Introduction

Most commercial polymer latex formulations contain between 40 to 55 vol% solids, the remainder being water and dissolved species. In order to reduce manufacturing costs and improve product quality, there is ongoing commercial interest in developing high solid content latexes that contain as much as 75 vol% solids. However such a formulation typically requires a well-defined particle size distribution (PSD) to maintain colloidal stability and provide an acceptable product viscosity.[1] The production of high solid content latexes is of ongoing academic interest, but the commercialization of such processes is further complicated by the fact that mixing is non-homogeneous in all but the smallest lab-scale reactors. The ability to anticipate and adapt to important changes in key process time and length scales can significantly reduce the costs of commercialization by reducing the amount of trial-and-error pilot plant experimentation required.

Computational fluid dynamics (CFD) provides a means of studying the important flow and mixing dynamics inside a wide range of vessel geometries and sizes, but incorporating a full kinetic model for PSD into the CFD simulation is, to our knowledge, impractical, even when one has access to high performance computing power. Fortunately, the kinetic model can be solved on a much coarser mesh without loss of detail.[2] One simple way to couple the CFD simulation and kinetic model together is to use them in a sequential manner by using the CFD hydrodynamics to generate a coarse mesh consisting of multiple zones, with each zone behaving as a well-mixed unit; therefore, a single PSD is solved in each zone. When operating in or

[1] Department of Chemical Engineering, Queen's University, Kingston ON, Canada
E-mail: tim.mckenna@chee.queensu.ca
[2] Research Unit on Industrial Flows Processes (URPEI) & Center for Applied Research on Polymers and Composites (CREPEC), Montreal, Quebec, Canada

near the transitional regime, as is the case in many latex reactors, the hydrodynamics may evolve significantly during the process as the viscosity of the latex changes; this necessitates the use of two-way coupling between CFD simulation and population balance models.

Elgebrandt et al.[3] adapted the general hybrid multizonal/CFD framework developed by Bezzo et al.[2,4] to emulsion polymerization, but they focused on the production of relatively dilute latexes while operating in the turbulent regime. This work focuses instead on laying the foundation for the development of a hybrid multizonal/CFD framework to capture the dynamics of the final production stages of high solid content (HSC) latexes. The highly non-Newtonian behaviour of the latexes in the laminar and low transition regimes is of particular interest. As this work is preliminary, the kinetic model has been restricted to controlled coagulation, a process that is employed in the production of polymer materials for a wide range of applications.[5]

Overview of the Simulation Framework

The simulation framework consists of three components: the multizonal population balance model, the CFD model and a set of interface routines to handle the generation of zones and the transmission of data between models. The mixing system that was modeled to demonstrate the framework was a tank with a four-bladed 45° pitched blade turbine and two round baffles. The reactor geometry is illustrated in Figure 1, along with key vessel and impeller dimensions.

An unstructured CFD mesh was generated in three dimensions using the Gambit (Ansys), a commercial pre-processor. The

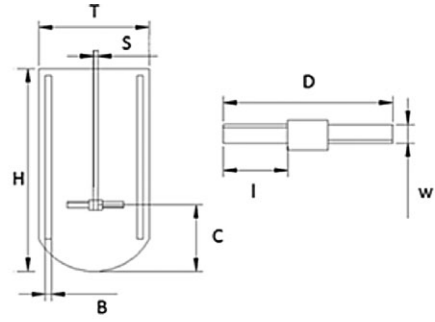

Part	Symbol	Relative Dimension
tank diameter	T	T
tank height	H	1.4 T
blade diameter	D	T/3
shaft diameter	S	T/30
baffle diameter	B	D/12
blade width	W	D/5
blade length	l	(7/15) D
blade clearance	C	H/3

Figure 1.
(left) three dimensional structure of the vessel including the main features; (right) schematic of the reactor geometry showing the dimensions of the key design parameters.

mesh was sufficiently refined in regions with large velocity gradients in order to provide sufficient resolution of the flow field (i.e. the mesh was refined until the computed power consumption converged). The presence of baffles in the tank will result in flow that is periodic in nature, although this effect is much stronger in the turbulent regime. A preliminary set of simulations was run to contrast the non-stationary flow fields generated with the fictitious domain method to the stationary flow field generated by imposing a rotational condition on the impeller surface. It was found that the periodic components of the non-stationary solution were minimal such that the stationary solution nearly matched the non-stationary solution; therefore, in order to minimize computation times, the stationary CFD model was used.

All CFD simulations were run using Poly3D (Rheosoft Inc.), a commercial 3D finite element method (FEM) code. The flow field was determined by solving the momentum and continuity equations with a standard 3D Galerkin FEM with the following boundary conditions:

- constant angular velocity along the impeller surface
- no slip condition at the baffles and along the vessel wall
- no normal velocity at the fluid surface which is assumed to be flat

The velocity and pressure fields were approximated using MINI finite elements, a type of element that has been shown to produce accurate flow fields at lower computational costs relative to other element types.[6] Post-Processing visualization was carried out using Paraview (Kitware), while key information (e.g. inter-zonal flow rates, corresponding zone number for each CFD element) was extracted from results files using a series of customized Fortran programs. The non-Newtonian rheology was modeled with the Carreau-Yasuda model which has been shown to correctly capture the shearing behaviour of concentrated latexes. Each of the four relevant parameters of the Carreau-Yasuda model (zero shear viscosity, infinite shear viscosity and the characteristic frequencies of shear thinning and thickening) are all functions of the latex solids volume fraction and the maximum packing fraction of the latex according to the general form of the Kreiger-Dougherty equation, leading to potentially a high degree of nonlinear coupling between the flow field and PSD. The details of the model, including the mechanistic model developed to calculate the maximum packing fraction as a function of the PSD shape are available in a previous publication[7] from our group.

It was assumed that the main cause of non-homogeneity within the tank is poor flow in the vertical tank (i.e. from the impeller region to the top and bottom of the tank). As this is a preliminary study of the framework, the zoning algorithm employed is somewhat primitive. The network-of-zones is generated by dividing the vessel into sections along its vertical axis, such that the net rate flow rate between any two neighbouring zones is zero (i.e. flow in = flow out). However the rate at which material is exchanged between zones is not zero; the rate of flow exchanged (i.e. flow in OR flow out) can be computed by projecting the normal components of the velocity field onto the interface. A distribution of axial flow exchange as a function of axial location is generated by calculating the rate of rate of flow exchange across 100 equally-spaced planes. This axial flow distribution, $F_L\ (z)$, and its maximum value $F_{L,max}$ are used to determine the appropriate spacing for the cut-off boundary values. Since the vessel is divided into an equal number of zones above and below the well-mixed impeller region, the number of cut-off boundary values required (n_{cutoff}) can be computed as follows:

$$n_{cutoff} = \frac{n_{zones}}{2} - 1 \tag{1}$$

where n_{zones} is the total number of zones to be generated. The cut-off boundary value for the central region was set to ($\log_{10}[F_L/F_{L,max}] = -0.75$) while the value for the

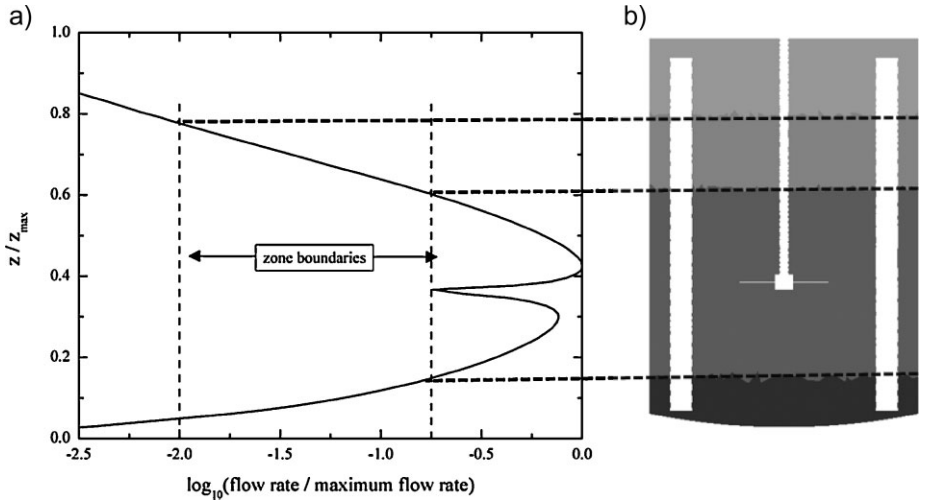

Figure 2.
(a) Rate of flow exchanged in the vertical direction along the height of a 1 L vessel, as determined from a preliminary CFD flow field (using the initial conditions described in the next section). The rate of exchange was rendered dimensionless using the maximum rate of flow exchange which is located in the vicinity of the impeller. (b) The tank was divided into five zones, using four horizontal cut-off boundaries (two above the region of maximum flow exchange and two below). This zoning procedure required two cut-off values of the dimensionless rate of flow exchange ($\log[F_L(z)/F_{L,max}]$ -0.75,-2.0). Note that the bottom-most zone was very thin to the other four zones and hence it is not shown in this diagram.

outermost boundaries was set at ($\log_{10}[F_L/F_{L,max}] = -2.0$). The remaining cut-off values are generated at equally-spaced ratios between the two limiting values. For $n_{zones} = 5$, no additional cut-off boundary values are generated. The resulting partitioning is illustrated in Figure 2.

multizonal model is comprised of a series of interconnected zones, each zone being modeled using one set of population balance equations. Following the fixed pivot technique developed by Ramkrishna et al.,[8] the discretized PBE is written as follows:

$$\begin{aligned}\frac{dN_{i,z}(t)}{dt} = & \sum_{\substack{j,k \\ (\overline{V}_{i-1}<(\overline{V}_j+\overline{V}_k)\le\overline{V}_i)}}^{i-1-j} (1-\frac{1}{2}\delta_{j,k})b(\overline{V}_j+\overline{V}_k,\overline{V}_i)\beta_{jk,z}N_{j,z}(t)N_{k,z}(t) \\ & + \sum_{\substack{j,k \\ (\overline{V}_i<(\overline{V}_j+\overline{V}_k)\le\overline{V}_{i+1})}}^{i-1-j} (1-\frac{1}{2}\delta_{j,k})a(\overline{V}_j+\overline{V}_k,\overline{V}_i)\beta_{jk,z}N_{j,z}(t)N_{k,z}(t) \\ & -N_{i,z}(t)\sum_{j=1}^{M}\beta_{ij,z}N_{j,z}(t) + \sum_{y,y\neq z}\left[N_{i,y}(V,t)-N_{i,z}(V,t)\right]Q_{z,y}\end{aligned} \quad (2)$$

The current kinetic model is restricted to controlled coagulation, which eliminates the particle nucleation and particle growth (via polymerization) terms from the population balance equation (PBE). The

where $N_{i,z}(t)$ is the number concentration of particles in with a pivot volume of $\overline{V}_i$ in zone z, $N_{i,z}(t)$ is the number of concentration of particles with pivot volume $\overline{V}_i$ in the neighbouring zone y, $\beta_{jk,z}$ is the coagulation

rate coefficient between particles of volumes $\overline{V}_i$ and $\overline{V}_j$, and $Q_{z,y}$ is the rate of flow exchanged between zones z and y. The population balance pivot points are not spaced in a constant interval; when a coagulation event produces a particle with a volume that falls between the pivot point values of $\overline{V}_{i-1}$ and $\overline{V}_i$ or $\overline{V}_i$ and $\overline{V}_{i+1}$, $a(\overline{V}_j + \overline{V}_k, \overline{V}_i)$ and $b(\overline{V}_j + \overline{V}_k, \overline{V}_i)$ are computed to determine what fraction of particles are assigned to the pivot point $\overline{V}_i$. Refer to Ramkrishna et al.[8] for a more detailed explanation of the numerical algorithm utilized. The population balance model was coded in Fortran and the solution for the resulting system of ordinary differential equations was computed with DLSODE, a general purpose explicit numerical scheme available for free download on the Netlib.[9]

Due to the small size of the particles, it is assumed that the dominant mechanism of coagulation is Brownian motion (perikinetic aggregation). A standard DLVO-based approach was used, in which it is postulated that the coagulation rate coefficient is dependent on the stability of the particle, indicated by the total particle potential energy of interaction. While there are limitations to the DLVO theory and the standard DLVO coagulation kernel, it is currently the only non-empirical model particle coagulation available.[10] The details of the coagulation kernel have been published elsewhere;[11,12] the most significant modification made to the standard coagulation kernel was the modification of the Debye parameter to account for a reduction in the thickness of the double layer at high solids concentrations.[13]

The manner in which all the elements communicate with each other is schematically depicted in Figure 3. The computational framework proceeds in the following steps:

1) At the start of the simulation, the contents of the vessel are assumed to be uniform. The initial flow field is calculated using viscosity model parameters that are calculated from the initial PSD.
2) The initial flow field is used to compute the axial location of the zoning partitions and the rate of exchange flow between zones.
3) The multizonal coagulation model is initialized.
4) The coagulation model proceeds until a large enough change in any of the viscosity model parameters in any of the zones is detected (thus signifying a strong possibility that the flow field has changed). The viscosity parameters used in the CFD model are re-computed using the Kreiger-Dougherty equation.

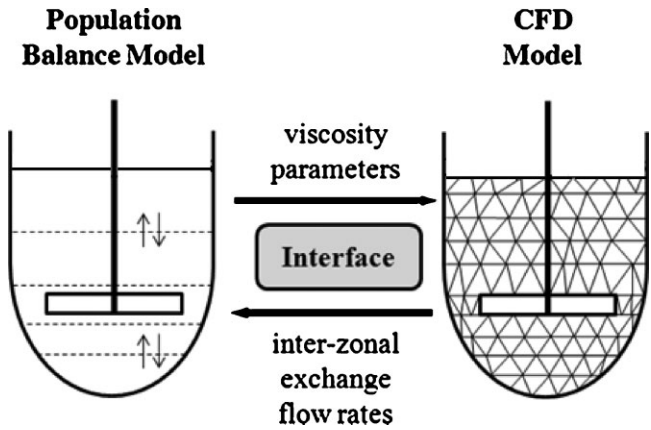

Figure 3.
Schematic diagram of the framework, outlining the path(s) of communication between the various framework components.

5) The flow field is updated via CFD simulation utilizing the updated viscosity parameters.
6) Steps 4 and 5 are repeated until the specified simulation end-time is reached.

Preliminary Results

To test the framework, a series of simulations were performed in which a concentrated polystyrene latex is coagulated via the continuous addition of a salt (an indifferent electrolyte). The initial latex has a mean diameter of 150 nm, a particle dispersity index of 1.10 (PDI, defined as the weight-averaged diameter divided by the number-averaged diameter) and a solids volume fraction of 0.59. The salt is fed into the vessel in the impeller region to maximize its dispersal throughout the vessel. The conditions were selected in order to ensure that the amount of coagulation would be insignificant if vessel was perfectly mixed, but very noticeable if the local concentration of coagulant exceeds a critical value (i.e. the narrow concentration band over which the rate of coagulation goes from negligible to very fast) in any of the zones. Three geometrically-similar reactor volumes were examined: 1L, 10L and 100L. The impeller rotational speed was adjusted to ensure a constant power-input-per-unit volume (P/V), as this is a popular heuristic when the objective is to ensure preservation of mixing quality. This approach entails that for an increase in volume by a factor of 10, the impeller rotational speed is reduced by a factor of 0.6 and the tank Reynolds number will increase by a factor of approximately 2.75. Based on the initial PSD, the approximate initial range of Reynolds numbers is 15 to 110 (the approximate cut-off between laminar and transition flow is a tank Reynolds number of 100).

In order to determine the number of subdivisions required to obtain a solution that is independent of the number of zones specified, a series of simulations were run (with the vessel size set to 1 L) in which the number of zones was varied from 5 to 11 in odd increments, as shown in Figure 4. It can be seen that the solution became grid-independent at nine zones under the current zoning scheme. The study was repeated at the 10 L and 100 L size scales, to ensure the number of zones required to

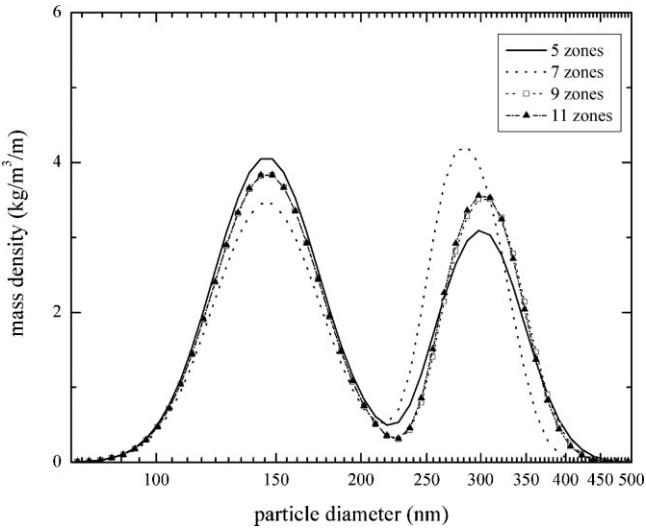

Figure 4.
Final PSD (obtained after adding 1.4 mol/L of electrolyte over a period of 215 seconds) as a function of the number of zones used in the population balance model. Simulations were carried out at the 1L scale.

achieve grid-independence remained constant independent of reactor scale. For a nine-zone system complete simulation times ranged from approximately 45 minutes to 90 minutes depending on the amount of fluid convection that had to be accounted for in the CFD simulations, and the frequency with which the flow field required updating (note that the criteria for updating the flow field were adjusted to ensure the final PSDs were convergent).

The change in the flow field with reactor scale can be assessed by examining the flow profile along the height of the vessel. The resulting axial flow distribution profiles are shown in Figure 5. It can be seen that the shape of the axial flow exchange profile evolves with reactor scale, indicating the introduction of inertial forces as the vessel is scaled-up. The presence of a large segregated region at the top of the vessel ($z/z_{max} > 0.8$) in all three cases indicates that mixing is poor in the upper portion of the vessel, regardless of the size of the reactor.

The key performance indicator within each zone of the vessel is the zonal mixing time ($\theta_{m,z}$), which is defined as:

$$\theta_{m,z} \equiv \frac{V_z}{\sum_{z,y \neq i} Q_{z,y}} \quad (3)$$

where V_z is the volume of zone z. Deep in the laminar regime where the flow field is independent of the tank Reynolds number, the zonal mixing will scale inversely by a factor of (1/D) where D is the vessel diameter. This is because the rate of flow exchanged at the zonal interfaces is proportional to the surface area of the interface, while zone volume scales directly with reactor volume. This is not the case when the flow field changes with vessel scale-up.

In Figure 6, the simulation conditions noted above were used to compare the final PSD obtained within a perfectly mixed reactor volume with the PSDs obtained in non-homogeneous and 1L and 10L vessels. The distribution obtained for a perfectly mixed system is included to show that poor mixing can have a drastic impact on the final PSD obtained during a coagulation process. The final PSDs obtained for the 1 L and 10 L vessel suggest that the process scales well between 1 L and 10 L reactors. The reduced surface area available for flow exchange between zones at 10 L may be offset by the increasing influence of fluid convection.

The original intent was to run a set of simulations at three vessel scales; however convergence was an issue at the 100 L scale

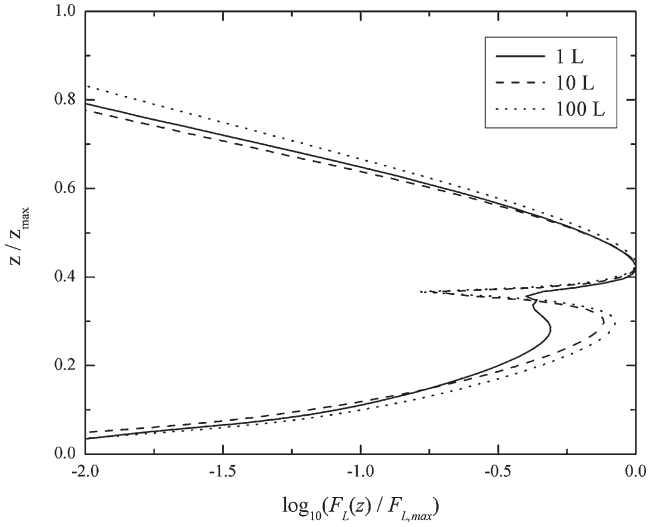

Figure 5.
Distribution of axial flow exchanged along the axial direction of the vessel at three tank volumes. Note that results are normalized to vessel height and the maximum rate of axial flow exchange.

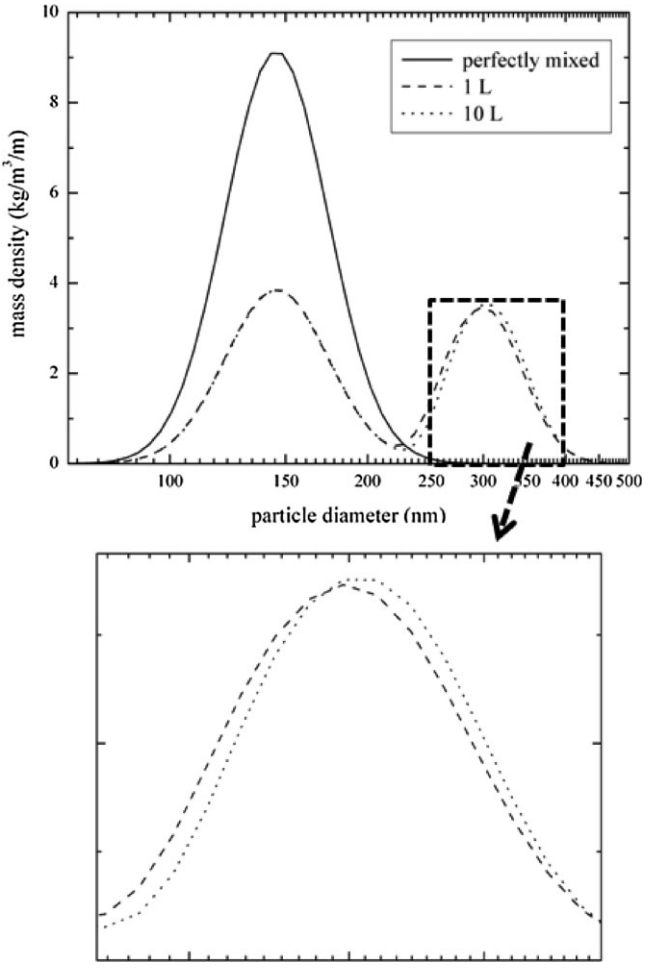

Figure 6.
Comparing the PSDs obtained at $t = 215$s in three vessels. The ''perfectly mixed'' vessel represents a reactor where conditions can be adjusted to ensure that the timescale of mixing is must faster than the time scale of particle coagulation.

when the flow field required updating. The coagulation of particles leads to a formation of a secondary population of larger particles. Considering a constant solids volume fraction, once the proportion of larger particles reaches a fraction of roughly 20%, the overall viscosity of the latex will begin to drop. When the initial PSD is specified near the maximum particle packing fraction, a broadening of the PSD can reduce latex viscosity by a factor of 10^2 (in fact, broadening the PSD is one technique employed to reduce the viscosity high solid content latexes). At the 100 L scale, this pushes operation further into the transition regime and possibly into the fully-turbulent regime (Re approaches 1000 – 10,000) and the CFD software was no longer capable of providing a solution. Limiting the study to reactor volumes less than 100 L is not an option as the ultimate intention is to develop a framework for scale-up that can predict performance at full commercial scale where tank volumes are often in the order of $10\,m^3$ or larger. The next logical steps toward improving the framework are to expand the kinetic model to a full emulsion polymerization model and to

integrate a second CFD code that is capable of predicting flow under turbulent conditions as was attempted previously by Elgebrandt et al.[3]

Conclusion

The hybrid multizonal/CFD computational framework outlined herein has the potential to become a strong predictive tool when assessing the feasibility of scaling up complex polymer latex processes, particularly those concerning the production of high solid content products. This preliminary set of simulations demonstrates that the framework can provide preliminary information regarding the quality of mixing inside a reactor and assess the impact of poor mixing on the quality of the final product. This preliminary information can guide the direction of pilot plant experimentation, reducing the time and cost commitments required to commercialize high solid content latexes. While the current framework is limited in scope to investigating particle coagulation in vessels operating in the laminar regime of mixing, further development of the framework is currently underway. The automatic zoning algorithm will be improved in an attempt to better-characterize the size and shape of the segregated regions in the vessel. Given the presence of turbulence in commercial vessels (and the onset of turbulence in vessels as small as 100 L in previous simulations), testing the framework in the turbulent regime via the integration of a turbulent CFD code is a priority, as is the incorporation of a complete emulsion polymerization model.

[1] M. Zubitur, J. M. Asua, *Polymer*, **2001**, *14*, 5979.
[2] F. Bezzo, S. Macchietto, C. C. Pantelides, *Comp. Chem. Eng.* **2004**, *4*, 501.
[3] R. C. Elgebrandt, D. F. Fletcher, V. G. Gomes, J. A. Romagnoli, "*16th European Symposium on Computer Aided Process Engineering and 9th International Symposium on Process Systems Engineering*", *W. Marquardt, C.C. Pantelides, Eds.*, *Elsevier B.V.*, 2006, p. 551–556.
[4] F. Bezzo, S. Macchietto, *Comp. Chem. Eng.* **2004**, *4*, 513.
[5] E. Kostansek, *Journal of Coatings Technology and Research* **2004**, *1*, 41.
[6] B. Coesnon, M. Heniche, C. Devals, F. Bertrand, P. A. Tanguy, *Int. J. Numer. Methods Fluids* **2008**, *4*, 427.
[7] M. Pishvaei, P. Cassagnau, T. F. McKenna, *Macromol. Symp.* **2006**, *1*, 63.
[8] D. Ramkrishna, "*Population Balances: Theory and Applications to Particulate Systems in Engineering*", Academic Press, London, UK 2000, p. 355.
[9] Anonymous, The Netlib Repository. http://www.netlib.org/.
[10] H. M. Vale, T. F. McKenna, *Prog. Polym. Sci.* **2005**, *10*, 1019.
[11] M. Fortuny, C. Graillat, T. F. McKenna, *Ind Eng Chem Res* **2004**, *23*, 7210.
[12] E. M. Coen, S. Peach, B. R. Morrison, R. G. Gilbert, *Polymer* **2004**, 3595.
[13] J. Eastman, "*Colloid Science*", T. Cosgrove, Ed., 2009, p. 36–49.

